# NUMERICAL SIMULATION OF FLOW OVER AIRFOIL USING ONE EQUATION TURBULENCE MODEL

**Marco Antonio Sampaio Ferraz de Souza, marco07@ita.br**
**José Casado Cáceres, jcaceres@ita.br**
**Nide Geraldo do Couto Ramos Fico Júnior, nide@ita.br**
Instituto Tecnológico de Aeronáutica - ITA
Divisão de Aeronáutica – Departamento de Aerodinâmica
Comando Geral de Tecnologia Aeroespacial – São José dos Campos – SP – Brasil

***Abstract.*** *It was developed a computational code to simulate the flow over a NACA0012 airfoil. Numerical simulation was performed to resolve the Reynolds-averaged Navier-Stokes (RANS) equations system that models a compressive turbulent flow. It was generated algebraically a structured "O" shape mesh and various refinements could be made. The differential equations system was discretized using the finite volume method and the Jameson explicit scheme was implemented. Artificial viscosity terms were added with a non-linear model. The one equation turbulence model of Spalart and Allmaras it was implemented to resolve the turbulence closing problem. At the beginning Euler formulation was used and we run cases of transonic inviscid flow over the airfoil. We compared the solutions with the results of other numerical methods found in the literature. Finally, the Spalart and Allmaras turbulence model was used for the Navier-Stokes formulation and the results were compared with experimental data of Harris and others numerical results got from the Baldwin and Lomax algebraic turbulence model.*

***Keywords****: computational fluid dynamics, finite volume method, turbulence model, compressible flow, airfoil.*

## 1. INTRODUCTION

Increasingly, the use of computational tools and simulations in aerodynamics has reduced the projects that use prototypes in real physical situations which tend to have higher costs like the wind tunnel tests. The growing capacity of processing and storage of computers in recent years is allowing a more detailed modeling of the problems and the use of more refined meshes.

The numerical solution in cases involving aerodynamic flow can begin when the laws that govern these processes are expressed in mathematical form in terms of differential equations.

The differential equations express the principle of conservation. Each equation uses a physical quantity as the dependent variable and means that there must be a balance between the various factors that influence the variable. The dependent variables of these equations typically represent specific properties and the terms in a differential equation of this type show an influence on volume (Patankar, 1980). A differential equation is a compilation of such terms, each representing an influence on a volumetric basis and all the terms together means a balance or conservation. The theoretical prediction of the physical phenomena of interest is governed by a system of differential equations. Therefore, it is necessary to develop ways to solve this system.

From the end of the eighties with the advent of supercomputers and constant increase in storage capacity and computational speed, it made possible the development of codes able to solve the Reynolds-averaged Navier-Stokes (RANS) equations. The process of averaging of the dependent variables is to divide them into two parts, one being the average in time and the other the fluctuation on the average, creating new terms known as the Reynolds stresses. To close the problem, it is necessary to develop ways to evaluate these new quantities. Thus it was created the models of turbulence. A common classification of models of turbulence is in accordance with the number of additional partial differential equations to be solved (Anderson, 1984). The simplest algebraic models are considered models of zero equation. The simplicity and low computational cost led to the popularization of algebraic models such as Cebeci and Smith (1974) and the Baldwin and Lomax (1978).

To achieve a more generalized application were developed turbulence models of one equation that adds a turbulent transport equation to the Reynolds-averaged Navier–Stokes equations like the models of Baldwin and Barth (1990) and Spalart and Allmaras (1992). All turbulence models have its limitations; this area is a major challenge within of Computational Fluid Dynamics (CFD). The latest works done to simulate numerically compressible turbulent flows over airfoils use algebraic turbulence models. This led the authors to develop a code based on finite volume method and implement the one equation turbulence model of Spalart and Allmaras to solve the system of Reynolds-averaged Navier–Stokes equations.

## 2. THEORETICAL FORMULATION

### 2.1. Fundamental Equations

The fundamental equations of fluid dynamics are based on the universal laws of conservation (Anderson, 1984):

1. Conservation of mass
2. Conservation of momentum
3. Conservation of energy

### 2.2 Navier-Stokes Equations

The nomenclature of the classical fluids mechanics refers to the Navier-Stokes equations as the equations of momentum for a Newtonian fluid. However, in CFD the terminology Navier-Stokes includes all the partial differential equations that model the flow field plus the constitutive relations needed.

### 2.3 Conservative form of Navier-Stokes equations

Formulations based on non-conservative partial differential equations can lead to numerical difficulties in situations where the coefficients may be discontinuous as in flows with shock waves. Therefore, it must develop the partial differential equations as conservative - or divergent - which has the property that the coefficients are all constant or, if variable, its derivatives do not appear in the equation (Anderson, 1984).

For a perfect gas without generating heat and disregarding field forces, the conservative form of Navier-Stokes equations using Einstein indicial notation can be written as:

$$\frac{\partial \rho}{\partial t} + \frac{\partial}{\partial x_i}\left(\rho u_i\right) = 0 \tag{1}$$

$$\frac{\partial}{\partial t}\left(\rho u_i\right) + \frac{\partial}{\partial xj}\left(\rho u_i u_j\right) = -\frac{\partial p}{\partial xi} + \frac{\partial}{\partial xj}\tau_{ij} \tag{2}$$

$$\frac{\partial e}{\partial t} + \frac{\partial}{\partial x_j}\left(e u_j\right) = \frac{\partial}{\partial x_j}\left(-p u_j + \tau_{ij} u_i - q_j\right) \tag{3}$$

where the viscous stresses tensor and the heat flux vector are given by

$$\tau_{ij} = \mu\left(\frac{\partial u_i}{\partial x_j} + \frac{\partial u_j}{\partial x_i}\right) - \frac{2}{3}\mu\frac{\partial u_k}{\partial x_k}\delta_{ij} \tag{4}$$

$$q_j = -k\frac{\partial T}{\partial x_i} \tag{5}$$

### 2.4 Reynolds Equations for turbulent flow

Although the Navier-Stokes equations model all the physics of the problem to be studied, capture all scales of turbulence that occur in the flow would need computational mesh so fine that would make the numerical solution prohibitive. What is usually done is leave the details and focus on the average values of properties. The result of this process is a system of equations known as Reynolds-averaged Navier–Stokes equations.

You can replace each variable by its two parcels in the Navier-Stokes equations and taking the mean of each equation, the resulting system is the Reynolds-averaged Navier–Stokes equations:

$$\frac{\partial \bar{\rho}}{\partial t} + \frac{\partial}{\partial x_j}\left(\bar{\rho}\tilde{u}_j\right) = 0 \tag{6}$$

$$\frac{\partial}{\partial t}\left(\bar{\rho}\tilde{u}_i\right) + \frac{\partial}{\partial xj}\left(\bar{\rho}\tilde{u}_i\tilde{u}_j\right) = -\frac{\partial \bar{p}}{\partial xi} + \frac{\partial}{\partial xj}\left(\bar{\tau}_{ij} - \overline{\rho u_i'' u_j''}\right) \tag{7}$$

$$\frac{\partial \bar{e}}{\partial t} + \frac{\partial}{\partial x_j}\left[(\bar{e}+\bar{p})\tilde{u}_j\right] = \frac{\partial}{\partial x_j}\left[\tilde{u}_i\left(\bar{\tau}_{ij} - \overline{\rho u_i'' u_j''}\right) + \overline{u_i''\left(\tau_{ij} - \frac{\rho u_i'' u_j''}{2}\right)}\right] - \frac{\partial \bar{q}_j}{\partial x_j} - \frac{\partial}{\partial x_j}\left(\overline{\rho u_j'' h}\right) \tag{8}$$

Compared to the Navier-Stokes equations in the original form, the new terms that appear, are the influence of turbulent fluctuations on the mean flow.

Therefore, it is necessary to shape the new terms to close the system of equations. Most models of turbulence based on the concept of effective viscosity of Boussinesq. The fundamental idea is to add to the molecular viscosity a coefficient of turbulent viscosity as follows:

$$\mu = \mu_l + \mu_t \tag{9}$$

It is assumed that the terms of Reynolds stress can be related to the flow medium in the same way that the tensor of viscous stress is related to the rate of deformation of a Newtonian fluid. You can then write the following relationship

$$\overline{\rho u_i'' u_j''} = \mu_t \left( \frac{\partial \tilde{u}_i}{\partial x_j} + \frac{\partial \tilde{u}_j}{\partial x_i} \right) - \frac{2}{3} \mu_t \frac{\partial \tilde{u}_k}{\partial x_k} \delta_{ij} \tag{10}$$

Similarly, adds to the molecular thermal conductivity a coefficient of turbulent thermal conductivity,

$$k = k_l + k_t \tag{11}$$

The turbulent thermal conductivity, $k_t$, is related to the turbulent viscosity, by the relationship:

$$\mathrm{Pr}_t = \frac{c_p \mu_t}{k_t} \tag{12}$$

Where $\mathrm{Pr_t}$ is the turbulent Prandtl number, which for the air, has a value $\mathrm{Pr_t} \approx 0.9$ (Bradshaw, Cebeci, 1981).

The turbulent viscosity, $\mu_t$, and turbulent thermal conductivity, $k_t$, are not properties of the fluid, unlike the molecular viscosity and thermal conductivity. Dependence of $\mu_t$ e $k_t$ on and the flow is the key difficult to model the turbulence. Introducing the hypothesis of Boussinesq, the equations (1), (2) and (3) can be written in terms of average quantities:

$$\frac{\partial \bar{\rho}}{\partial t} + \frac{\partial}{\partial x_j} \left( \bar{\rho} \tilde{u}_j \right) = 0 \tag{13}$$

$$\frac{\partial}{\partial t} \left( \bar{\rho} \tilde{u}_i \right) + \frac{\partial}{\partial x_j} \left( \bar{\rho} \tilde{u}_i \tilde{u}_j + \bar{p} \delta_{ij} - \tilde{\tau}_{ij} \right) = 0 \tag{14}$$

$$\frac{\partial \tilde{e}}{\partial t} + \frac{\partial}{\partial x_j} \left[ (\tilde{e} + \bar{p}) \tilde{u}_j - \tilde{\tau}_{ij} \tilde{u}_i + \tilde{q}_j \right] = 0 \tag{15}$$

And the tensor of viscous stresses and the vector of heat flux are now given by:

$$\tilde{\tau}_{ij} = (\mu_l + \mu_t) \left( \frac{\partial \tilde{u}_i}{\partial x_j} + \frac{\partial \tilde{u}_j}{\partial x_i} \right) - \frac{2}{3} (\mu_l + \mu_t) \frac{\partial \tilde{u}_k}{\partial x_k} \delta_{ij} \tag{16}$$

$$\tilde{q}_j = -\left( \frac{c_p \mu_l}{\mathrm{Pr}} + \frac{c_p \mu_t}{\mathrm{Pr}_t} \right) \frac{\partial \tilde{T}}{\partial x_i} \tag{17}$$

**2.5 Vector form of equations**

Before applying a finite volume algorithm to the fluids dynamics equations it is convenient to write the equations in a compact vector form. Therefore, the Reynolds-averaged Navier–Stokes equations, in the conservative form, in two-dimensional Cartesian coordinates, can be written in the following way:

$$\frac{\partial Q}{\partial t}+\frac{\partial E}{\partial x}+\frac{\partial F}{\partial y}=0 \tag{18}$$

Where $Q$ is the vector of conserved variables and $E$ and $F$ are the vectors of flow in the directions x and y, respectively, given by:

$$Q=\begin{Bmatrix}\overline{\rho}\\ \overline{\rho}\tilde{u}\\ \overline{\rho}\tilde{v}\\ \overline{e}\end{Bmatrix},\ E=\begin{Bmatrix}\overline{\rho}\tilde{u}\\ \overline{\rho}\tilde{u}^2+\overline{p}-\overline{\tau}_{xx}\\ \overline{\rho}\tilde{u}\tilde{v}-\overline{\tau}_{xy}\\ \left(\overline{e}+\overline{p}\right)\tilde{u}-\tilde{u}\overline{\tau}_{xx}-\tilde{v}\overline{\tau}_{xy}+\overline{q}_x\end{Bmatrix},\ F=\begin{Bmatrix}\overline{\rho}\tilde{v}\\ \overline{\rho}\tilde{u}\tilde{v}-\overline{\tau}_{xy}\\ \overline{\rho}\tilde{v}^2+\overline{p}-\overline{\tau}_{yy}\\ \left(\overline{e}+\overline{p}\right)\tilde{v}-\tilde{v}\overline{\tau}_{yy}-\tilde{u}\overline{\tau}_{xy}+\overline{q}_y\end{Bmatrix}. \tag{19}$$

It is usual to split the flow vector in term of inviscid and viscous parts as follows:

$$E=E_e-E_v,\quad F=F_e-F_v. \tag{20}$$

Where the subscript *e* represents the inviscid components for the Euler equations and the subscript *v* represents viscous components to be used in the Navier-Stokes equations.

### 2.6 Dimensionless form of the Navier-Stokes equations

The equations of fluid dynamics are often placed in dimensionless form. The advantage is that the flow variables are normalized so that their values are placed between certain limits prescribed such as zero and one. From the numerical point of view, this tends to reduce the spread of errors, since all the variables will be of the same order of magnitude. Moreover, the characteristic parameters such as Mach number, Reynolds number, Prandtl number, can be varied independently (Anderson, 1984).

## 3. NUMERICAL IMPLEMENTATION

To obtain the discretization equations from the partial differential equations system, the finite volume method uses the control volume formulation.

### 3.1 Form integral of the Navier-Stokes equations

We define the vector $\vec{P}$ as:

$$\vec{P}=E\vec{i}_x+F\vec{i}_y \tag{21}$$

Where *E* and *F* are the flow vectors defined by equation (19), $\vec{i}_x$ and $\vec{i}_y$ are the unit Cartesian vectors. The equation (18) can then be written as:

$$\frac{\partial Q}{\partial t}+\vec{\nabla}.\vec{P}=0 \tag{22}$$

Integrating the equation (22) for all unit control volumes we obtain:

$$\frac{\partial Q_{i,j}}{\partial t}=-\frac{1}{V_{i,j}}\int_{S_{i,j}}\left(\vec{P}\cdot\vec{n}\right)dS \tag{23}$$

Where $V_{i,j}$ is the volume of a cell and $S_{i,j}$ is the corresponding control volume surface.

### 3.2 The Jameson scheme

The Jameson (1986) finite volume formulation used in this work employ a Runge-Kutta integration scheme of five stages to march in time. The method has a fourth order accuracy in time and second order in space. The properties are evaluated as the average of the values in the cells on both sides of the face. Thus, the scheme reduces to an approximation of a space centered difference on a Cartesian mesh. As a result, it requires the use of terms of numerical dissipation to ensure stability (Jameson, 1981). The terms of artificial viscosity are evaluated at all stages of the Runge-Kutta scheme to increase the stability (Arias Garcia, 2006). Thus, adding the terms of artificial viscosity, we obtain:

$$\frac{dQ_{i,j}}{dt}+\frac{1}{V_{i,j}}\left[T_e\left(Q_{i,j}\right)-Da\left(Q_{i,j}\right)\right]=0 \tag{24}$$

Where $Da\left(Q_{i,j}\right)$ is the artificial viscosity term and $T_e\left(Q_{i,j}\right)$ is the discrete approximation of all the fluxes crossing the surface of the control volume, $V_{i,j}$.

### 3.3 Initial Conditions

The initial conditions must be set to start the iterative process. In this case, we use the properties values of the non-disturbed flow throughout the computational grid.

### 3.4 Boundary Conditions

One of the most important tasks of a numerical simulation is the correct implementation of the boundary conditions. Basically, we can define three types of boundaries for the flow over the NACA 0012 airfoil which we resolved in this work: solid wall, remote and symmetrical boundaries. As it is a two-dimensional case, four conditions at each boundary are necessary to resolve the problem.

### 3.5 Spalart and Allmaras turbulence model

The aerodynamics community is willing to invest in a new generation of turbulence models, more expensive than the algebraic models, but with a broader range in terms of flow and complexity of the mesh. In the Spalart and Allmaras one equation model, one transport equation for turbulent viscosity is assembled using empiricism and arguments of dimensional analysis, Galilean invariance, and a selective dependence on molecular viscosity (Spalart, Allmaras, 1992). The equation includes a term of not viscous destruction that depends on the distance to the wall. Unlike algebraic models and the first models of one equation, this is local in the sense that the equation in one point does not depend on the solution of a point elsewhere. It is therefore compatible with any mesh structure. The solution near the wall is less difficult. The conditions of wall and non-disturbed flow are trivial. The model produces laminar-turbulent transition relatively smooth, at specified points by the user. A simple turbulence index is provided to determine the regions of boundary layer where the model is enabled. The terms of transition have been deactivated, taking into consideration the fully turbulent flow. The model was calibrated in boundary layers with gradients of pressure. The turbulent viscosity is given by:

$$\nu_t=\rho\tilde{\nu}f_{v1} \tag{25}$$

Where

$$f_{v1}=\frac{\chi^3}{\chi^3+c_{v1}^3}, \qquad \chi\equiv\frac{\tilde{\nu}}{\nu} \tag{26}$$

$\nu$ is the molecular viscosity and $\rho$ is the local density. The variable of Spalart-Allmaras, $\tilde{\nu}$, follows the following transport equation:

$$\frac{\partial\tilde{\nu}}{\partial t}+\frac{\partial\left(\tilde{\nu}u_j\right)}{\partial x_j}=c_{b1}\tilde{S}\tilde{\nu}+\frac{1}{\sigma}\left[\nabla.\left(\left(\nu+\tilde{\nu}\right)\nabla\tilde{\nu}\right)+c_{b2}\left(\nabla\tilde{\nu}\right)^2\right]-\left[c_{w1}f_w\right]\left[\frac{\tilde{\nu}}{d}\right] \tag{27}$$

Since

$$\tilde{S} \equiv S + \frac{\tilde{\nu}}{k^2 d^2} f_{v2}, \qquad f_{v2} = 1 - \frac{\chi}{1 + \chi f_{v1}}, \tag{28}$$

$d$ is the distance to the nearest wall and $S$ is the magnitude of vorticity given by:

$$S \equiv \left(2\Omega_{i,j}\Omega_{i,j}\right)^{\frac{1}{2}}, \tag{29}$$

Where

$$\Omega_{i,j} = \frac{1}{2}\left(\frac{\partial u_i}{\partial x_j} - \frac{\partial u_j}{\partial x_i}\right). \tag{30}$$

The function $f_w$ is given by:

$$f_w = g\left[\frac{1 + c_{w3}^6}{g^6 + c_{w3}^6}\right]^{\frac{1}{6}}, \tag{31}$$

Where

$$g = r + c_{w2}\left(r^6 - r\right) \quad \text{and} \quad r \equiv \frac{\tilde{\nu}}{\tilde{S}k^2 d^2}. \tag{32}$$

The constants used in the model are:

$$\sigma = \frac{2}{3}, \quad c_{b1} = 0.1355, \quad c_{w1} = \frac{c_{b1}}{k^2} + \frac{\left(1 + c_{b2}\right)}{\sigma}, \quad c_{w3} = 2,$$
$$k = 0.41, \quad c_{b2} = 0.622, \quad c_{w2} = 0.3, \quad c_{v1} = 7.1. \tag{33}$$

The boundary conditions are established defining values of $\tilde{\nu}$. The wall condition is $\tilde{\nu} = 0$.

## 4. RESULTS

### 4.1 Euler Formulation for transonic flow over a NACA 0012 airfoil profile

The problem was solved using a structured mesh type "O" around the airfoil. The mesh contains 189x43 points. The external boundary is located at a distance of 20 chords of the profile and all the lengths were turn into dimensionless by the chord of the airfoil.

In all cases, the initial conditions were considered the values of the properties of non-disturbed flow, defined as:

$$p_\infty = 101325 \text{ N/m}^2,\ \rho_\infty = 1.223 \text{ kg/m}^3,\ a_\infty = 340.2 \text{ m/s},\ \gamma = 1.4.$$

The boundary condition in of the wall airfoil is the condition of slipping in the case of the Euler formulation. The model of nonlinear artificial viscosity was used for all cases. The numerical convergence criterion was established for a maximum density equal to $1\times10^{-9}$.

The results for the pressure coefficients $C_p$ are compared with other numerical results available in literature and we show the pressure profile and Mach number around the airfoil for each case. In this phase, the angle of attack $\alpha$ was varied up to two degrees to ensure that the flow is always glued to the surface of the airfoil and do not occur any regions of separation.

### 4.1.1 Case 1, $M_\infty = 0.8$ and $\alpha = 1.25^o$

In the first case was performed a simulation of a transonic flow with Mach number $M_\infty = 0.8$ and with an angle of attack $\alpha = 1.25°$. A strong shock wave appears in the airfoil upper camber and other weaker appears in the lower camber. The distribution of pressure shown in Fig. 1 is compared with the work of Oliveira, Kroll and Jain apud Oliveira. The results presented in this work are in good agreement with those presented by Oliveira, and Kroll and Jain. The pressure contours and Mach number for a region near the airfoil are shown in Fig. 2. Figure 3 shows the numerical convergence curve where the stopping criterion of the program was achieved in 35424 iterations.

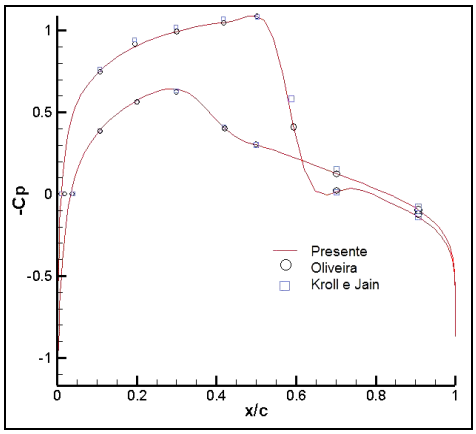


Figure 1: Comparison of Cp along the chord of the airfoil for $M_\infty = 0.8$ and α=1.25°.

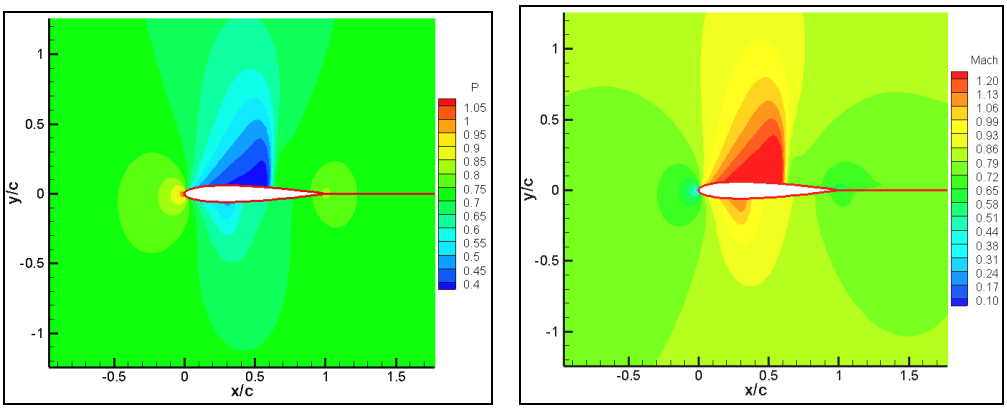


Figure 2: Contours of pressure and Mach number for $M_\infty = 0.8$ and α=1.25°

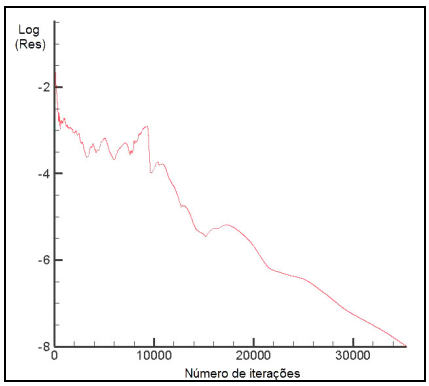


Figure 3: Curve of numerical convergence for $M_\infty = 0.8$ and α=1.25°.

### 4.1.2 Case 2, $M_\infty = 0.85$ and $\alpha = 1.0°$

The second simulation was performed for a transonic flow with Mach number $M_\infty = 0.85$, and an angle of attack $\alpha = 1.0°$. The pressure distribution on the airfoil shown in Fig. 4 is compared with the work of Oliveira and Kroll and Jain. Again, the results presented in this work are in good conformity with those presented by Oliveira, and Kroll and Jain. The pressure contours and Mach number for a region near the airfoil are shown in Fig. 5. Figure 6 shows the curve where the numerical convergence criterion for stopping the program was achieved in 40,660 iterations.

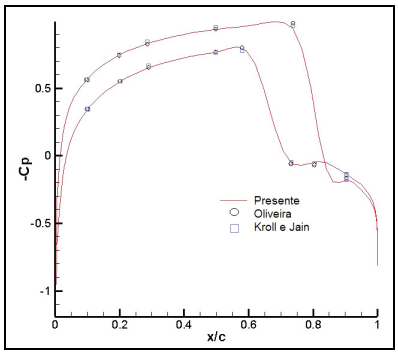


Figure 4: Comparison of Cp along the chord of the airfoil for $M_\infty = 0.85$ and α= 1.0 °

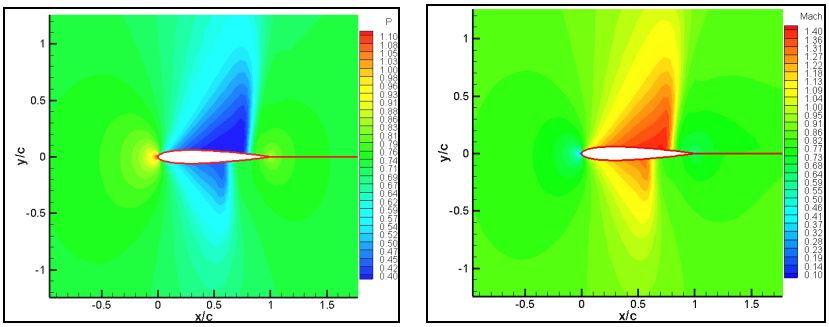


Figure 5: Curves of pressure and Mach number for $M_\infty = 0.85$ and α= 1.0 °

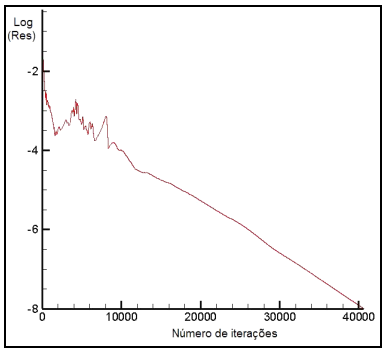


Figure 6: Numerical curve of convergence for $M_\infty = 0.85$ and α= 1.0 °

### 4.2 Formulation of Navier-Stokes for compressible turbulent flows over a NACA 0012 airfoil profile

To simulate the viscous turbulent flow over NACA 0012 airfoil was added the one equation turbulence model of Spalart and Allmaras to the code developed. The applied Spalart and Allmaras turbulence model was developed from the version of the work of Castro (2001). The terms of transition have been deactivated, taking into consideration the fully turbulent flow. The meshes were refined near the wall of airfoil as shown in Fig. 7 to capture the viscous effects in the region of the boundary layer. The code of Spalart and Allmaras model requires that the nearest point on the wall is at $y^+ \approx 1$ (Spalart, Allmaras, 1994).

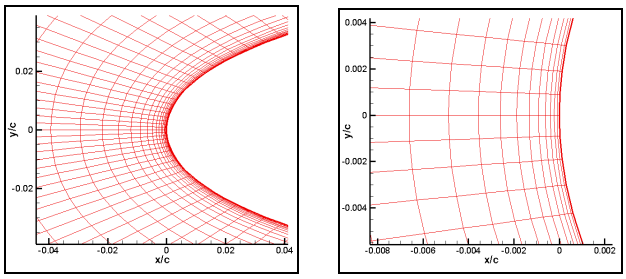


Figure 7: Refinement of the mesh near the leading edge of NACA 0012 airfoil.

The mesh used contains 189x43 points. The explicit scheme of Jameson was used for both cases with a CFL number equal to 0.2.

Flow on the NACA 0012 airfoil is widely used as reference in CFD, because of the large number of experimental data available. Two cases were simulated for different Reynolds numbers, Mach numbers and angles of attack. The solutions were compared with experimental data of Harris (1981) and numerical results obtained by Arias Garcia (2006) using the algebraic turbulence model of Baldwin and Lomax.

### 4.2.1 Case 1, Reynolds $3\times10^6$, $M_\infty = 0.5$ and $\alpha = 5.86°$

The first simulation for a turbulent flow case was made with Reynolds number of $3\times10^6$, Mach number $M_\infty = 0.5$ and angle of attack $\alpha$ = 5.86°. The chord for this Reynolds and Mach numbers is 0.2767 m. The pressure distribution shown in Fig. 8 is compared with the experimental data of Harris and the numerical solution obtained by Arias Garcia using the algebraic turbulence model of Baldwin and Lomax. As shown in Fig. 8, the pressure coefficient distribution along the airfoil using the Spalart and Allmaras turbulence model is closer to the experimental data of Harris than the algebraic model of Baldwin and Lomax. Comparing with the experimental data, $C_n$ = 0.626, the coefficient of normal force obtained with the Spalart and Allmaras model was $C_n$ = 0.629. This is less than 0.5% of error, while the error obtained with the Baldwin and Lomax model was close to 1%. The curves of pressure and Mach number for a region near the airfoil are shown in Fig. 9. Figure 10 shows the curve of numerical convergence where the criterion for stopping the program was achieved in 24951 iterations.

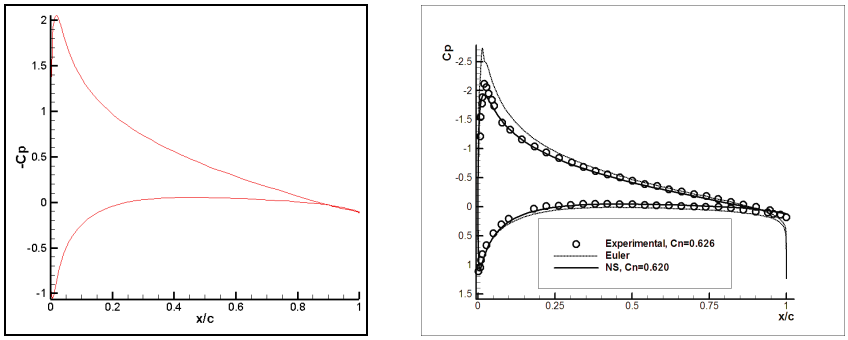


Figure 8: Distribution of pressure coefficient $M_\infty$ = 0.5 and $\alpha$ = 5.86. (a) Present work and (b) Arias Garcia.

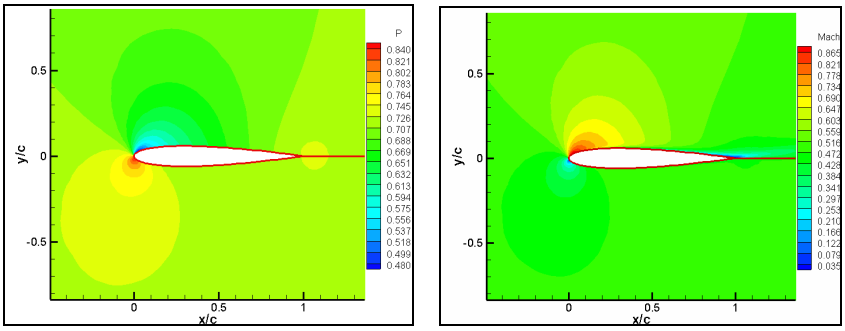


Figure 9: Curves of pressure and Mach number for $M_\infty$ = 0.5 and $\alpha$ = 5.86.

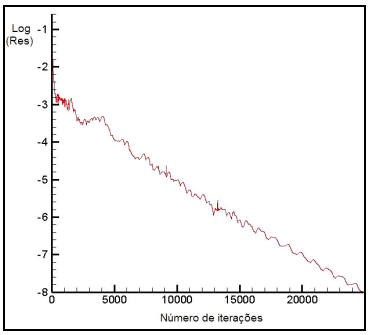


Figure 10: Curve of numerical convergence for $M_\infty$ = 0.5 and $\alpha$ = 5.86

### 4.2.2 Case 2, Reynolds $9\times10^6$, $M_\infty = 0.74$ and $\alpha = -0.14°$

The second simulation to turbulent case was performed for a flow with Reynolds number equal to $9\times10^6$, Mach number $M_\infty = 0.74$ and angle of attack $\alpha$ =- 0.14°. The chord for this Reynolds and Mach numbers is 0.56 m. The distribution of pressure, shown in Fig. 11 is compared with the experimental results of Harris and the numerical solution obtained by Arias Garcia using the algebraic turbulence model of Baldwin and Lomax showing good conformity between the results. The curves of pressure and Mach number for a region near the airfoil are shown in Fig. 12. Figure 13 shows the curve of numerical convergence where the criterion for stopping the program was achieved in 38,332 iterations. Here, the coefficient of normal force obtained with the Spalart and Allmaras model, $C_n$ = 0.020, was the same as the experimental data of Harris and the solution found using the Baldwin and Lomax model.

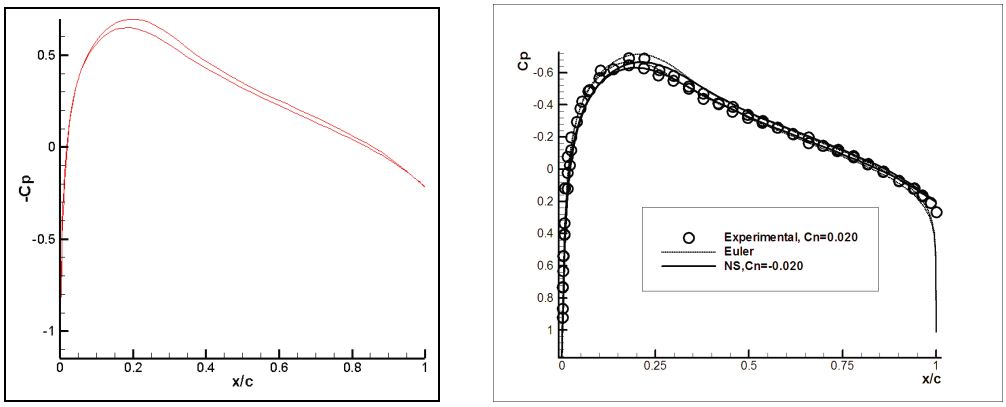


Figure 11: Distribution of pressure coefficient for $M_\infty$ = 0.74 and $\alpha$ = -0.14. (a) Present work and (b) Arias Garcia.

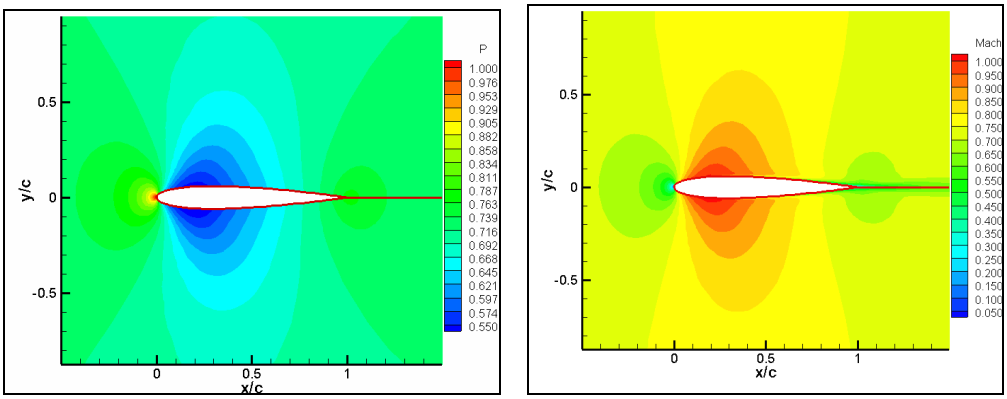


Figure 12: Curves of pressure and Mach number for $M_\infty$ = 0.74 and $\alpha$ =-0.14

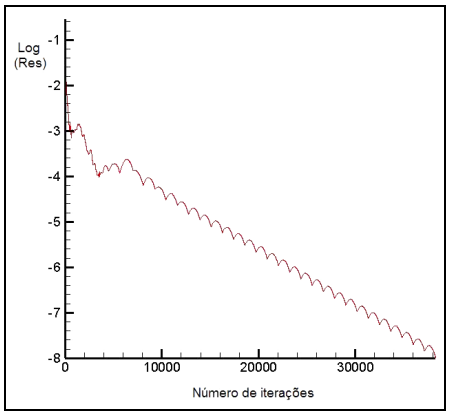


Figure 13: Curve of numerical convergence for $M_\infty$ = 0.74 and $\alpha$ =-0.14

## 5. CONCLUSION

The Spalart and Allmaras one equation turbulence model was implemented numerically to close the Reynolds-averaged Navier–Stokes (RANS) equations that model the compressible turbulent flow over a NACA 0012 airfoil. Despite being more expensive than the algebraic models, the Spalart and Allmaras one equation model has a broader range in terms of flow and complexity of the mesh. The finite volume method was used to discretize the partial differential equations system and the Jameson explicit scheme was implemented. Initially, the Euler formulation was used and results for the pressure distribution were obtained for two cases of non-viscous transonic flow on the airfoil. The solutions were compared with other numerical methods available in the literature and showed good conformity between the results. Finally, the Spalart and Allmaras one equation turbulence model was used for the Navier-Stokes formulation and the solutions were compared with experimental data of Harris and other numerical solutions obtained from the algebraic turbulence model of Baldwin and Lomax presenting good conformity between the results.

## 6. REFERENCES

Anderson, D. A., Tannehill, J. C., Pletcher, R. H., 1984, *Computational fluid mechanics and heat transfer*, New York: McGraw-Hill.

Arias Garcia, O. M., 2006, *Numerical simulations of compressible flows over airfoils*.137 f. Thesis of master of sciencies – Aeronautics Institute of Technology, São José dos Campos.

Baldwin B. S., Barth, T. J., 1990, *A one-equation turbulence transport model for high Reynolds number wall-bounded flows*, NASA TM 102847.

Baldwin, B. S.; Lomax, H., 1978, *Thin layer approximation and algebraic model for separated turbulent flows*, AIAA paper 78-257, AIAA 16th AEROSPACE SCIENCES MEETING, Huntsville, Alabama.

Bradshaw, P.; Cebeci, T., Whitelaw, J. H., 1981, *Engineering calculation methods for turbulent flow*, Academic Press, London.

Castro, B. M., 2001, *Multi-Block Parallel Navier-Stokes Simulation of Unsteady Wind Tunnel and Ground Interference Effects*, Naval Posgraduate School, Monterey, California.

Cebeci, T., Smith, A. M. O., 1974, *Analysis of turbulent boundary layers*, Academic Press, London.

Harris, C., D., 1981, *Two-dimensional aerodynamic characteristics of the NACA 0012 airfoil in the langley 8 foot transonic pressure tunnel*. Langley Research Center: NASA. (NASA Technical Memorandum, 81927).

Jameson, A., Mavriplis, D., 1986, *Finite volume solution of the two-dimensional Euler equations on a regular triangular mesh*, AIAA Journal, vol. 24, No.4, pp. 611-618.

Jameson, A., Schimidt, W., Turkel, E., 1981, *Numerical solution of the Euler Equations by finite volume methods using runge-kutta time-stepping schemes.* In: FLUID AND PLASMA DYNAMICS CONFERENCE, 14, Palo Alto. Palo Alto: AIAA. Paper No.81-1259

Johnson, D. A., King, L.S., 1985, *A Mathematically simple turbulence closure model for attached and separated turbulent boundary layers*, AIAA Journal, vol. 23-11, pp. 1684-1692.

Kroll, N.; Jain, R. K., 1987, *Solutions of the two-dimensional Euler equations – experience with a finite volume code*, DFVLR-FB 87-41.

Oliveira, L. C., 1993, *Uma metodologia de análise aeroelástica com variáveis de estado utilizando técnicas de aerodinâmica computacional*. 100 f. Dissertação de Mestrado - Instituto Tecnologico de Aeronáutica, São Jose dos Campos.

Patankar, S. V.,1980, *Numerical heat transfer and fluid flow*, Washington: Hemisphere Publishing Corporation.

Spalart, P. R., Allmaras, S. R., 1992, *A one-equation turbulence model for aerodynamic flows*. In: 30th AEROSPACE SCIENCES MEETING & EXHIBIT, 1992, Reno. Proceedings... Reno: AIAA. (AIAA-92-0439)
Spalart, P. R., Allmaras, S. R., 1994, *A one-equation turbulence model for aerodynamic flows*, La Recherche Aérospatiale, No. 1, pp. 5-21.

## 7. RESPONSIBILITY NOTICE

The authors are the only responsible for the printed material included in this paper.